

# A patient-specific visualization tool for comprehensive analysis of coronary CTA and perfusion MRI data

H.A. Kirişli<sup>a,b</sup>, V. Gupta<sup>b,c</sup>, S. Kirschbaum<sup>d</sup>, L. Neefjes<sup>d</sup>, R.J. van Geuns<sup>d</sup>, N. Mollet<sup>d</sup>,  
B.P.F. Lelieveldt<sup>b,c</sup>, J.H.C.Reiber<sup>b</sup>, T. van Walsum<sup>a</sup> and W.J. Niessen<sup>a,e</sup>

<sup>a</sup>Biomedical Imaging Group Rotterdam, Dept. of Medical Informatics, Erasmus MC, Rotterdam, the Netherlands

<sup>b</sup>Division of Image Processing, Dept. of Radiology, Leiden UMC, Leiden, the Netherlands

<sup>c</sup>ICT Group, Department of Mediamatics, Delft Univ. of Technology, Delft, the Netherlands

<sup>d</sup>Dept. of Cardiology & Radiology, Erasmus MC, Rotterdam, the Netherlands

<sup>e</sup>Imaging Science & Technology, Faculty of Applied Sciences, Delft Univ. of Technology, Delft, the Netherlands

## ABSTRACT

Cardiac magnetic resonance perfusion imaging (CMR) and computed tomography angiography (CTA) are widely used to assess heart disease. CMR is used to measure the global and regional myocardial function and to evaluate the presence of ischemia; CTA is used for diagnosing coronary artery disease, such as coronary stenoses. Nowadays, the hemodynamic significance of coronary artery stenoses is determined subjectively by combining information on myocardial function with assumptions on coronary artery territories. As the anatomy of coronary arteries varies greatly between individuals, we developed a patient-specific tool for relating CTA and perfusion CMR data. The anatomical and functional information extracted from CTA and CMR data are combined into a single frame of reference. Our graphical user interface provides various options for visualization. In addition to the standard perfusion Bull's Eye Plot (BEP), it is possible to overlay a 2D projection of the coronary tree on the BEP, to add a 3D coronary tree model and to add a 3D heart model. The perfusion BEP, the 3D-models and the CTA data are also interactively linked. Using the CMR and CTA data of 14 patients, our tool directly established a spatial correspondence between diseased coronary artery segments and myocardial regions with abnormal perfusion. The location of coronary stenoses and perfusion abnormalities were visualized jointly in 3D, thereby facilitating the study of the relationship between the anatomic causes of a blocked artery and the physiological effects on the myocardial perfusion. This tool is expected to improve diagnosis and therapy planning of early-stage coronary artery disease.

**Keywords:** Computed Tomography Angiography (CTA), Cardiac Magnetic Resonance perfusion imaging (CMR), Coronary Artery Disease (CAD), diagnosis, visualization.

## 1. INTRODUCTION

Coronary artery disease (CAD) is one of the major causes of death in the world<sup>1</sup>. Oxygen and nutrients, which are required for a normal heart function, are supplied to the myocardium (e.g. the heart muscle) by the blood traveling through the coronary arteries. If a coronary artery becomes narrowed or blocked with plaque buildup (e.g. cell, fat and cholesterol), the amount of blood flowing to the myocardium is reduced and, thus, less oxygen and nutrients are delivered to these myocardium regions. This lack of blood and oxygen is called ischemia. Coronary artery narrowing and blockage can either cause temporary changes to these under-supplied areas or, if the myocardium is not supplied by enough blood during a too long period, cause death of the heart tissue, which may lead to a heart-attack.

Many tests are available for detecting and diagnosing coronary artery diseases, such as electrocardiography, exercise stress tests, nuclear scan tests, stress thallium and cardiac catheterization. The choice of which test to perform is determined by the patient's history and current symptoms. If coronary artery disease is diagnosed, there are many ways to treat it, such as life style changes (e.g. daily activity, stopping smoking and changes in diet) or medication. If life-style changes and

---

Further author information: H.A. Kirişli  
E-mail: h.kirisli@erasmusmc.nl, Telephone: +31-10-7044246, <http://www.bigr.nl/people/HortenseKirisli>.

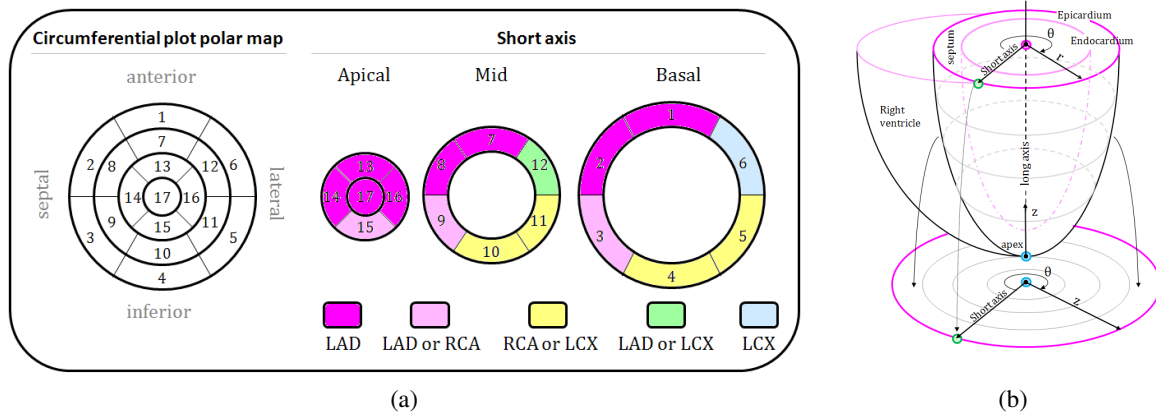


Figure 1. (a) Correspondence of left ventricular 17 myocardial segments with each coronary artery according to Pereztol *et al.*<sup>4</sup> results. - (b) Common frame of reference - Our Bull's Eye Plot (BEP) is a 2D representation of the myocardium. It is constructed by unfolding and reformatting the 3D myocardium to a circle. (cf. Termeer *et al.*<sup>5</sup>).

medication are not effective, more invasive procedure may be considered, such as balloon angioplasty or bypass graft surgery.

Currently, X-ray angiography is the gold standard imaging technique for diagnosing CAD, with which the location, the number and the severity of the blockages can be determined. Nevertheless, Computed Tomography Angiography (CTA), a non-invasive imaging technique, is gaining in popularity as an alternative. Coronary artery stenoses (e.g. narrowing/blockage of the artery) can be visualized on CTA, e.g. using multi-planar reformatted (MPR) or maximum intensity projection (MIP) images.

To determine which therapy would be the most effective for a patient, the location and the information regarding the severity of the stenosis may not be sufficient; additional information about the myocardium may be required. Cardiac Magnetic Resonance perfusion imaging (CMR) is one of the imaging technologies that can be used to measure the global and regional myocardial function of the heart and to evaluate the presence of ischemia<sup>2</sup>. Conventionally, the interpretation of left ventricular abnormalities is performed either by visually checking the cardiac MR perfusion sequences (under rest and stress) or by looking at the perfusion parameters, using the standardized 17-segment Bull's Eye Plot (BEP) model of the American Heart Association (AHA)<sup>3</sup>.

In current clinical practice, the cardiologist independently views the CTA (i.e. using MPR/MIP images of the vessels) and CMR perfusion images (i.e. using rest/stress sequences and BEP representation). Subsequently, the hemodynamic significance of coronary artery stenoses is determined subjectively, by mentally combining information on myocardial function with assumptions on coronary artery territories<sup>3</sup>. Pereztol *et al.*<sup>4</sup> demonstrated that only nine of the 17 AHA-segments are fed by a single coronary artery, while the eight other segments may be fed by more than one coronary artery (Figure 1(a)); this is explained by the high variability of the coronary anatomy between patients. Therefore, if a patient has more than a single vessel obstructed and if the degrees of the stenoses are similar, the physiological effect of a particular stenosis may be difficult to determine. Thus, neither the anatomical nor the functional information alone is sufficient; a patient-specific combination of both information can be necessary.

Various visualization tools that propose image fusion to combine coronary anatomy with myocardial physiology have already been proposed in the literature: Faber *et al.*<sup>6</sup> proposed a method to integrate the information from biplane X-ray angiograms and perfusion SPECT, while Gaemperli *et al.*<sup>7</sup> suggested to fuse CTA with SPECT myocardial perfusion imaging. Termeer *et al.*<sup>5</sup> proposed a comprehensive visualization framework (called CoViCAD) to relate whole-body and perfusion MRI data. The distinction of our work with Termeer's is that Termeer extracted coronary centerlines from MR images, whereas we obtained the complete coronary tree segmentation from CTA images. Another approach related to our own work is proposed by Oeltze *et al.*<sup>8</sup> and Kuehnle *et al.*<sup>9,10</sup>, who integrate anatomical and physiological data from CTA and MRI images respectively. However, they do not provide a mapping of the coronary arteries integrated in the 2D BEP.

In this work, we present a patient-specific tool for comprehensive analysis of coronary CTA and CMR perfusion data. This work combines visualization techniques used in the previously proposed method (e.g. Termeer *et al.*<sup>5</sup>, Oeltze *et al.*<sup>8</sup> and Kuehnel *et al.*<sup>9,10</sup>): CTA data are used to analyse coronary arteries and an interactive BEP with coronary arteries overlaid is used to correlate the anatomical and dynamic image information. Such a tool is expected to improve diagnosis and therapy planning of early-stage coronary artery disease.

## 2. METHOD

### 2.1 CTA images processing

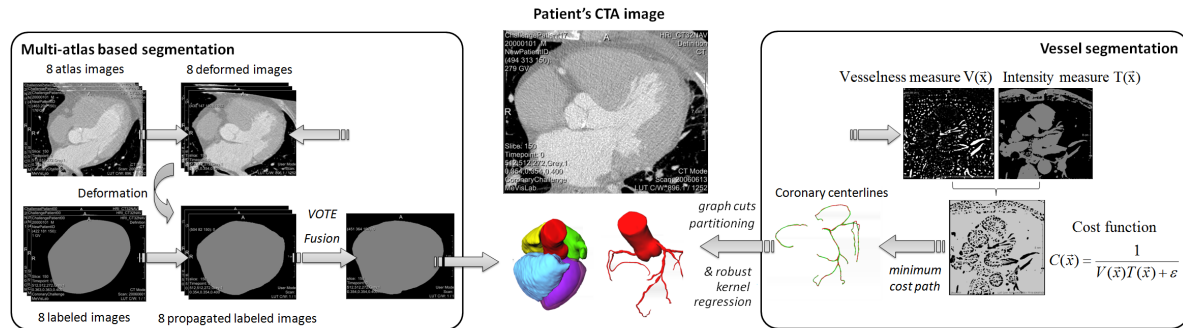


Figure 2. Overview of the CTA image processing

Computed Tomography Angiography imaging (CTA) provides information regarding the presence, extent, and type (noncalcified or calcified) of coronary plaques. In daily clinical practice, CTA images are evaluated using different visualization techniques, such as multiplanar reformatting and curved planar reformatting images, both of which require the centerline of the vessel of interest.

In this work (see Figure 2), a semi-automatic method<sup>11</sup> was used to extract vessel centerlines: a minimum cost path approach was applied, in which the user interaction was minimized to one or two mouse clicks in the coronary arteries. First, a vesselness/intensity cost function was computed. Then, a point in the aorta close to the coronary ostia was detected automatically and used as a start-point; an end-point was then defined by the user distally, at the end of the coronary artery. The centerline was determined by following the path of steepest descent to the starting point of the artery. Finally, the resulting centerline was used in combination with a graph cuts partitioning and a robust kernel regression to achieve the coronary lumen segmentation<sup>12</sup>. This step was followed by visual inspection and manual refinement of the lumen segmentation was performed where needed.

In addition, a 3D model of the heart, which includes ventricles, atria and aorta, was derived automatically from CTA data using a multi-atlas based segmentation approach<sup>13</sup>. Such a 3D model of the heart was useful for supporting user's orientation and localization.

### 2.2 Cardiac MR perfusion images processing

Cardiac perfusion magnetic resonance imaging (CMR) provides information about myocardial perfusion. In clinical practice, physiologically relevant features, together with their time-intensity behavior, are extracted from the CMR images, which require tracking of regional myocardial intensity in all the frames of a perfusion sequence as a function of time.

In this work (see Figure 3), a fully automatic framework<sup>14</sup> was used to analyze the CMR perfusion images. First, because the intensity signal must be derived from the same myocardial region in successive frames, the CMR perfusion images were compensated for respiratory motion using a registration method based on Independent Component Analysis<sup>15</sup> (ICA).

Subsequently, the registered data were used to automatically segment the myocardium with active appearance models. Finally, given the myocardium segmentation, time-intensity curves and perfusion parameters were computed, such as the baseline signal intensity (signal intensity value before the first-pass of the contrast-agent), peak-enhancement (PE) or

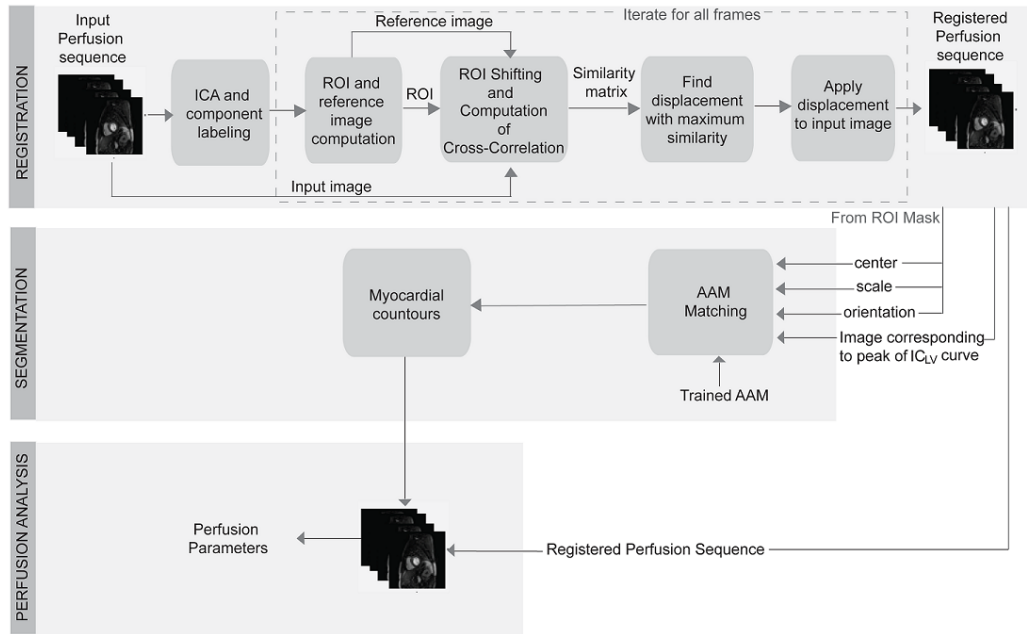


Figure 3. Overview of the CMR image processing

amplitude (maximal signal intensity value normalized by the baseline value), mean intensity (mean intensity during the first-pass of contrast-agent), time to (50%) of PE (time between the start of the first-pass and the time at which (50%) of PE is achieved), upslope (maximum steepness during the first-pass of contrast-agent) and Myocardial Perfusion Reserve Index (MPRI) (ratio of the up-slope at stress to the up-slope at rest).

### 2.3 Combination of CTA and CMR data

To combine information extracted from CTA and from CMR perfusion data, both data first need to be spatially aligned. In this work, we used an iterative closest point (ICP) approach, in which an affine transformation is determined. The ICP algorithm requires a set of data points  $p \in P$  (i.e. points from CMR epicardial contours) and a set of target points  $q \in Q$  (i.e. points from the 3D CTA epicardium model). The transformation is initialized by aligning both centers of gravities; this results in two new sets of points  $P_0$  and  $Q_0$ . Given a user-defined maximum number of iterations ( $N = 100$ ) and/or a maximum distance ( $\epsilon = 1.10^{-5}$ ) as stopping criterion, the iterative procedure will search for the affine transformation that minimizes the distance between each  $p \in P_i$  and  $q \in Q_i$ ,  $P_i$  and  $Q_i$  being the set of points after the  $i^{th}$  iteration.

Then, a common frame of reference<sup>5</sup> (Figure 1(b)), based on the segmentation of the left ventricle, was used to combine the information extracted from the CTA and from the CMR perfusion data. Each point of the coronary vessel centerlines was parameterized using cylindrical coordinates  $(r, \theta, z)$ . In this parameterization,  $\vec{z}$  represents the left ventricle long-axis;  $\theta$  represents the angle with the short-axis; and  $r$  represents the distance to the long-axis. In our 2D BEP representation, the radius corresponds to the  $z$  value, the angle to the  $\theta$  values. The third dimension, corresponding to the  $r$  parameter, is encoded in the rendering: the more transparent the artery is, the more far it is from the left ventricle epicardium surface.

### 2.4 Visualization & Interaction

Our graphical user interface has been developed under MeVisLab and examples are shown in Figures 4 to 7.

First, the basic tools used in daily clinical practice are present in our GUI. The vessel of interest (e.g. selected in our vessel list) can be visualized using both short (left) and long (right) cross-sectional views of the curve planar reformatted CTA images. Also, the rest/stress CMR perfusion images and their corresponding time-intensity curves are available.

In addition to these standard visualization tools, two viewers allow the comprehensive analysis of the data. A 3D viewer (top left) displays the 3D model of the heart and of the coronaries, with an option of color-coded radius. A 3D model of

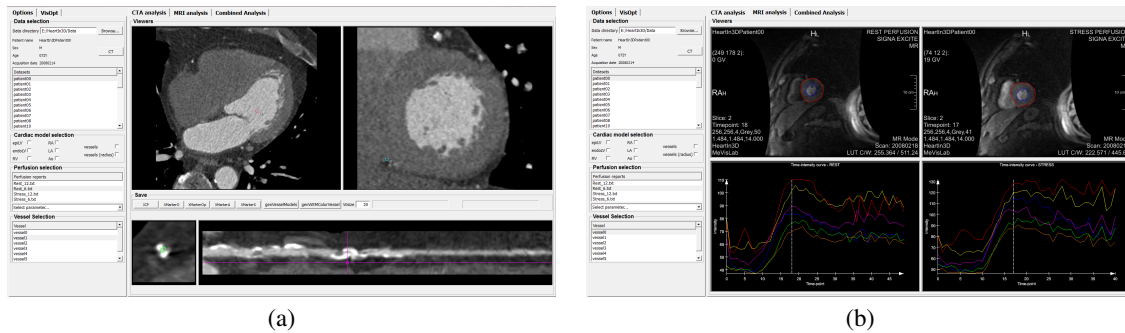


Figure 4. (a) CTA analysis GUI panel - Axial view of CTA data (top left), short-axis reformatted view (top right), CPR view of the selected vessel (bottom) - (b) CMR perfusion GUI panel - Rest/stress CMR perfusion data (top), rest/stress time-intensity curves (bottom). On the left side, there are 2 panels: 1) to navigate in the data (change patient, display patient information and reports, select specific artery, specific perfusion parameter ...) and 2) to control the visualization (change perfusion color, display heart model, show 2D/3D viewers, overlap coronary arteries on 2D BEP, add clip-planes,...).

the BEP segments, color-coded with the user-selected perfusion parameter, can be displayed and CTA clip-planes can be added. Such an overlay provides a direct 3D correspondence between the vessel and the myocardial region supplied by the vessel. A 2D BEP representation (top right) is available, with the option of overlapping the coronary arteries. The radius of the vessel can also be color-coded to improve stenosis visualization and detection. Furthermore, a 2D/3D interaction is available between the viewers: if the user moves the cursor along the centerline on the long cross-sectional MPR view, the corresponding short cross-sectional MPR view is updated and a white cross indicates the position of the cursor along the centerline on both the 2D and 3D viewers.

### 3. EXPERIMENTS & RESULTS

#### 3.1 Data

CTA and CMR perfusion data were acquired in the Erasmus MC, University Medical Center Rotterdam, the Netherlands. We retrospectively obtained data of 14 patients (11 males, 3 females), ranging from 48 to 72 years in age ( $63 \pm 7.2$  y.o.), who underwent both cardiac CTA and MRI examinations, between October 2007 and April 2008.

CTA images were acquired with a dual-source CT scanner (Somatom Definition, Siemens Medical Solutions, Forchheim, Germany). A tube voltage of 120 kV was used. All datasets were acquired with ECG-pulsing. Diastolic reconstructions were used, with reconstruction intervals varying from 250 ms to 400 ms before the R-peak. The data were reconstructed using a smooth (B26f) kernel. The mean voxel size of the datasets is  $0.32 \times 0.32 \times 0.4 \text{ mm}^3$ .

All the CTA data were evaluated by radiologists and vessel lesions were scored visually ( $< 50\%$ ,  $> 50\%$  or  $100\%$ ). A stenosis was considered significant if the stenosis diameter was larger than 50% of the vessel diameter. Multi-vessel disease was defined as the presence of a significant lesion in at least two epicardial vessels in different perfusion territories. Of our 14 patients, three had a single-vessel disease in LAD, six had double-vessel disease and five had triple-vessel disease. Two patients had a total occlusion of one vessel. Table 1 shows the repartition of the vessel disease per patient.

CMR perfusion images were acquired using a 1.5 Tesla scanner with a cardiac eight-element phased-array receiver coil placed over the thorax (Signa CV/i, GE Medical systems, Milwaukee, Wisconsin USA). Cine cardiac MRI was performed with a steady-state free precession technique (FIESTA). Repeated breath holds and gating to the electrocardiogram were applied to minimize the influence of cardiac and respiratory motion on data collection. During a breath hold, the extra vascular contrast media, gadolinium diethytriaminepentaacetic acid (Magnevist, Schering, Germany) was injected via an intravenous catheter ( $0.05 \text{ mmol/kg}$  at  $3 \text{ ml/sec}$ ; Medrad). Its first pass was monitored using a presaturation scheme with a notched excitation followed by a segmented gradient echo/echo-planar read out with the following imaging parameters: field of view  $32 - 36 \times 32 - 36 \text{ cm}$ , rectangular field of view 0.75, repetition time 6.8 ms, echo time 2.0 ms, inversion time 150-175 ms, preparation pulse  $90^\circ$ , time to echo 1.2 ms, train length 4, number of averages 0.75, bandwidth 125 kHz, flip angle  $20^\circ$ , matrix 128/96, slice thickness 6-8 mm, slice gap 2-4 mm. The temporal resolution per slice of 120 ms allowed imaging of 3-5 slices per R-R interval. Perfusion imaging was planned to cover the basal mid and apical part of the left ventricle. Fifteen minutes after rest perfusion vasodilatation was induced by adenosine ( $140 \mu\text{g/kg/min}$  body weight over

Table 1. List of patients and their respective vessel disease. The vessel is considered as disease if more than 50% of the vessel is occluded (significant stenosis) - LAD = left anterior descending artery; LCX = left circumflex artery; RCA = right coronary artery; LM = left main coronary artery; IMB = intermediate branch; MO = marginal obtuses; D1/D2 = diagonales branches; \* = complete occlusion.

	Vessels								Vessel disease
	LAD	LCX	RCA	LM	IMB	MO	D1	D2	
p00	> 50%	< 50%	< 50%	< 50%	> 50%			> 50%	double
p01	> 50%	> 50%	> 50%			> 50%			triple
p02	> 50%	< 50%	< 50%	< 50%		> 50%	< 50%	< 50%	double
p03	> 50%						> 50%	> 50%	single
p04			> 50%	> 50%					double
p05	> 50%						> 50%	> 50%	single
p06	> 50%	< 50%	> 50%	< 50%	> 50%				triple
p07	> 50%	> 50%	> 50%	< 50%	> 50%				triple
p08	> 50%	100%	> 50%	< 50%		100%		> 50%	triple*
p09	> 50%	> 50%	< 50%						double
p10	> 50%		> 50%				> 50%		double
p11	> 50%	> 50%	> 50%						triple
p12	> 50%					< 50%		< 50%	single
p13	> 50%	< 50%	100%						double*

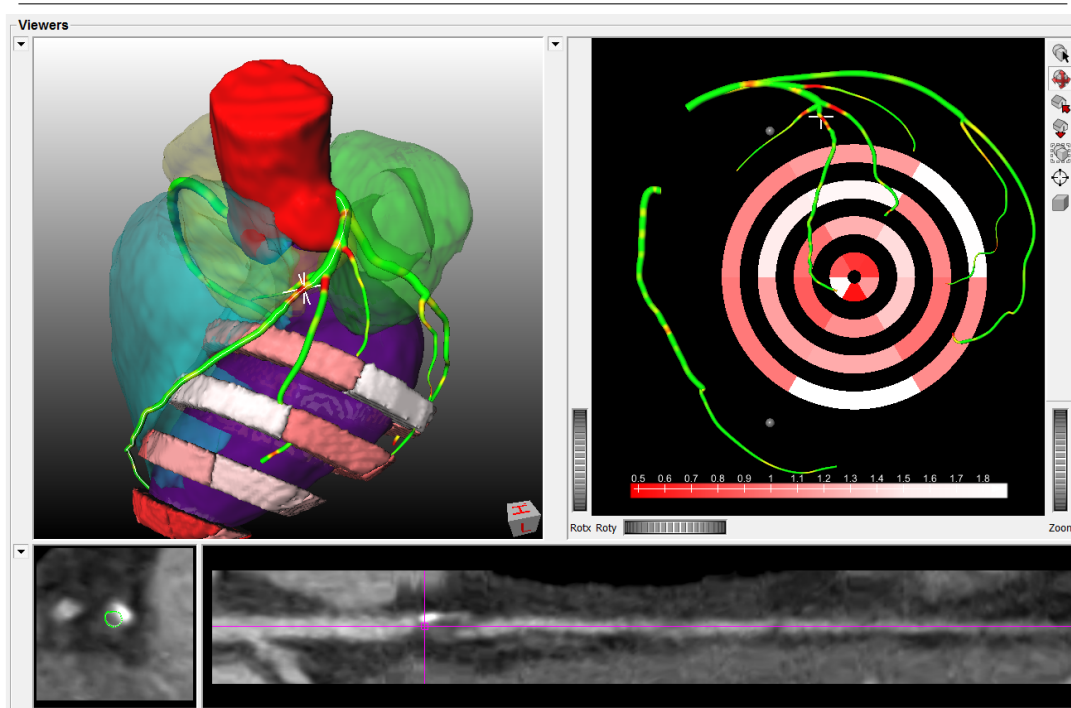


Figure 5. Analysis of a patient with single vessel disease (53 y.o. woman) : patient p05, LAD and diagonal branches have significant stenosis (> 50%) - Myocardial perfusion reserve index is shown on the bull's eye plot, range from 0.5 (red) to 1.9 (white).

3 minutes) a second bolus of gadolinium diethyl-triamine-penta-acetic acid was injected via the intravenous catheter (0.05 mmol/kg at 3 ml/sec) and stress first pass perfusion images were acquired using the same pulse sequence and the same orientations used for rest perfusion.

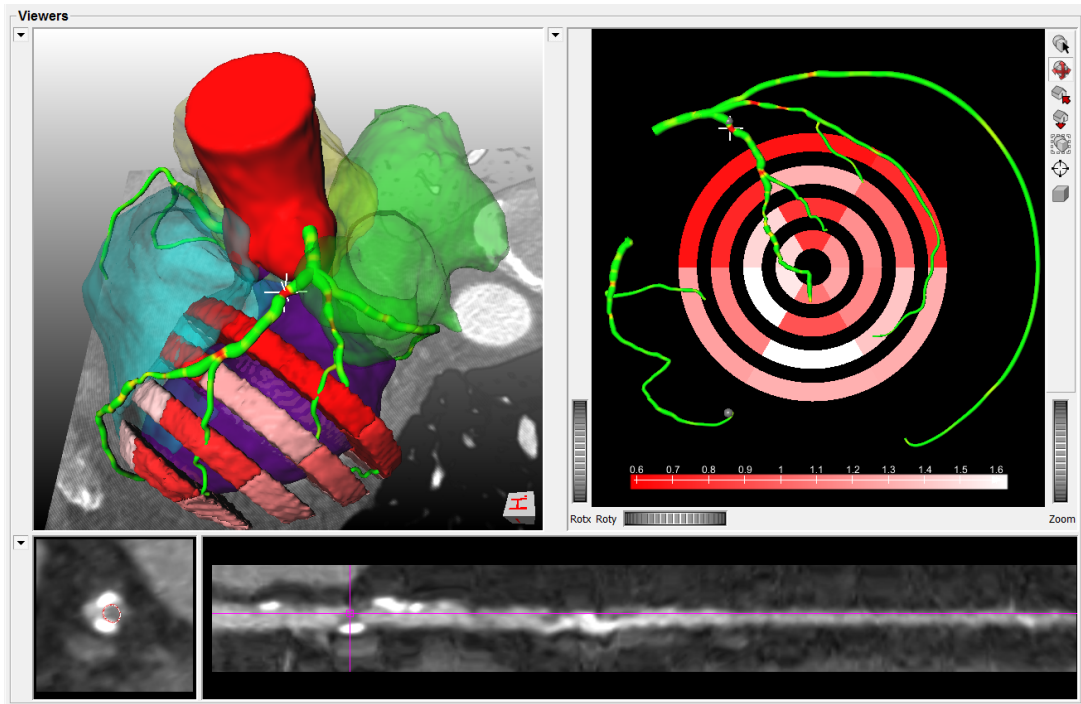


Figure 6. Analysis of a patient with double vessel disease (72 y.o. man): patient p00, LAD and IMB have significant stenosis ( $> 50\%$ ) - Myocardial perfusion reserve index is shown on the bull's eye plot, range from 0.6 (red) to 1.6 (white).

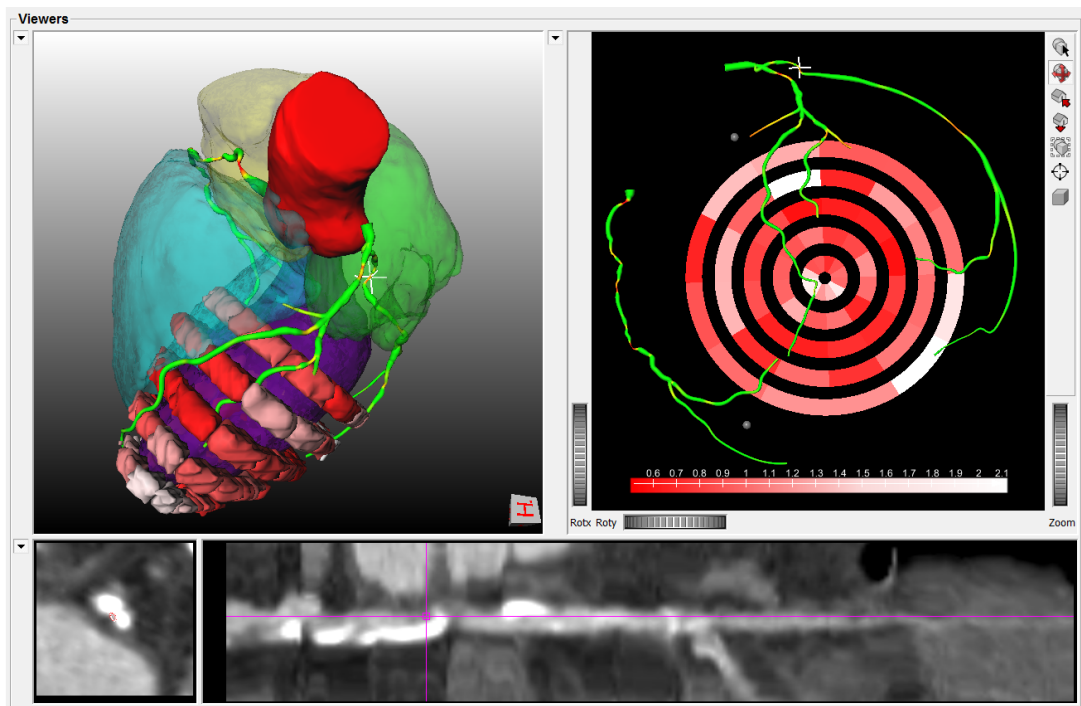


Figure 7. Analysis of a patient with triple vessel disease (64 y.o. man): patient p11, RCA, LAD and LCX have significant stenosis ( $> 50\%$ ) - Extensive coronary artery disease - Myocardial perfusion reserve index is shown on the bull's eye plot, range from 0.5 (red) to 2.1 (white).

### 3.2 Results

The integrated visualization and analysis of CMR perfusion and CTA data has been applied to data of 14 patients. Figures 5 to 7 show results for one single-, one double- and one triple-vessel disease patient respectively. Similar results were obtained for the other patients.

The myocardial perfusion reserve index (MPRI) is represented on the BEP. It has been demonstrated<sup>16</sup> that an MPRI of 1.5 is a good cutoff value between ischemic and normal myocardial segments. The stenosis might induce a perfusion defect in patient-specific myocardial regions.

In the case of the *first patient* (53 y.o. woman, p05 in Table1), who suffers from single-vessel disease with mixed plaques and significant stenoses (> 50%) in the LAD and in the diagonal branches, the myocardial perfusion reserve index does not show any significant differences between myocardial segments supplied by stenotic coronary arteries and nonstenotic coronary arteries, except at the apex. Thus, the myocardial segments supplied by LAD and diagonal branches seem to not be affected yet by the restriction of perfusion due to stenoses.

In the case of the *second patient* (72 y.o. man, p00 in Table1), who suffers from double-vessel disease with mixed plaques and significant stenoses in the LAD and intermediate branches, the spatial relationship between the stenoses and perfusion defects can effectively be shown in the combined visualizations. In fact, the basal anterior, anteroseptal, anterolateral, and mid anteroseptal segments present significant differences in myocardial perfusion reserve after stress infusion, which correspond to the significant stenoses detected in LAD and IMB. The inferior and inferolateral segments being also supplied by LCX, it seems that the LAD stenosis should be treated in priority to reperfused the anteroseptal wall, which is exclusively supplied by LAD.

In the case of the *third patient* (64 y.o. man, p11 in Table1), who suffers from triple-vessel disease and extensive coronary artery disease with mixed plaques and significant stenoses in the 3 main coronaries, it is difficult to relate a certain myocardial region to a specific coronary artery, due to the extent of the disease. Using a higher resolution BEP (e.g. with more segments) might help to determine if there is a myocardial region more underperfused than other one.

## 4. DISCUSSION / CONCLUSION

We presented an integrated visualization approach that allows to effectively and efficiently establish a spatial correspondence between diseased coronary artery segments and myocardial regions with abnormal perfusion. The location of coronary stenoses and perfusion abnormalities were visualized jointly in 2D and 3D, thereby facilitating the study of the relationship between the anatomic causes of a blocked artery and the physiological effects on the myocardial perfusion.

As a future work, we would like to investigate the possible role of our visualization tool in diagnosing coronary artery disease in clinical practice and evaluate the clinical benefit. We will perform a case study evaluation to answer the following research question: 'How can our visualization tool, which combines information about coronary arteries and myocardial perfusion, assist radiologists in studying the hemodynamic significance of stenosis and in making coronary artery disease (CAD) diagnosis?'. Interviews of both young ( $\leq 3$  years experience) and expert ( $\geq 10$  years experience) radiologists/cardiologists will take place: few single-, double- and triple-vessel disease patients will be analyzed by the radiologist/cardiologist using the visualization tool and case propositions will be answered.

In conclusion, although the full value for diagnosis and therapy planning remains to be investigated both on a larger number of cases and in clinical environment, our initial results demonstrate that the integrated multimodal visualization has large potential to improve clinical workflow in the assessment of CAD.

## 5. ACKNOWLEDGMENTS

The research leading to this publication was supported by a grant from the Dutch Ministry of Economic Affairs (AgentschapNL) under the title "Het Hart in Drie Dimensies" (PID06003) <http://www.bigr.nl/heartin3d>.

## REFERENCES

- [1] Association, A. H., "Heart disease and stroke statistics - 2010 update: A report from the american heart association," *Circulation* (2010).
- [2] Kirschbaum, S. and van Geuns, R., "Cardiac magnetic resonance imaging to detect and evaluate ischemic heart disease," *Hellenic Journal of Cardiology* **50**, 119–126 (2009).
- [3] Cerqueira, M. and AHA, "Standardized myocardial segmentation and nomenclature for tomographic imaging of the heart," *Circulation* **105**, 539–542 (2002).
- [4] Pereztol-Valdés, O., Candell-Riera, J., Santana-Boado, C., Angel, J., Aguadé-Bruix, S., Castell-Conesa, J., Garcia, E., and Soler-Soler, J., "Correspondence between left ventricular 17 myocardial segments and coronary arteries," *European Heart Journal* **26**(24), 637–2643 (2005).
- [5] Termeer, M., Bescós, J., Breeuwer, M., Vilanova, A., Gerritsen, F., and Gröller, M., "Covicad: Comprehensive visualization of coronary artery disease," *IEEE Trans. on Visualization and Computer Graphics* **13**(6), 1632–1641 (2007).
- [6] Faber, T., Santana, C., Garcia, E., Candell-Riera, J., Folks, R., Peifer, J., Hopper, A., Aguade, S., Angel, J., and Klein, J., "Three-dimensional fusion of coronary arteries with myocardial perfusion distributions: Clinical validation," *Journal of Nuclear Medicine* **45**(5), 745–753 (2004).
- [7] Gaemperli, O., Schepis, T., Kalf, V., Namdar, M., Valenta, I., Stefani, L., Desbiolles, L., Leschka, S., Husmann, L., Alkadhi, H., and Kaufmann, P., "Validation of a new cardiac image fusion software for three-dimensional integration of myocardial perfusion SPECT and stand-alone 64-slice CT angiography," *Eur J Nucl Med Mol Imaging* **34**, 1097–1106 (2007).
- [8] Oeltze, S., Kub, A., Hennemuth, A., and Preim, B., "Integrated visualization of morphologic and perfusion data for the analysis of coronary artery disease," *Eurographics IEEE VGTC Symposium on Visualization*, 131–138 (2006).
- [9] Kühnel, C., Hennemuth, A., Oeltze, S., Boskamp, T., and Peitgen, H., "Enhanced cardio vascular image analysis by combined representation of results from dynamic MRI and anatomic CTA," in [*Proc. SPIE Medical Imaging*], **6918** (2008).
- [10] Kühnel, C., Hennemuth, A., Peitgen, H., and Mahnken, A., "New analysis tools for the comprehensive assessment of the coronary arteries and myocardial viability in CT data sets," *Computers in Cardiology* **35**, 733–736 (2008).
- [11] Metz, C., Schaap, M., Weustink, A., Mollet, N., van Walsum, T., and Niessen, W., "Coronary centerline extraction from CT coronary angiography images using a minimum cost path approach," *Medical Physics* **36**(12), 5568–5579 (2009).
- [12] Schaap, M., Neefjes, L., Metz, C., van der Giessen, A., Weustink, A., Mollet, N., Wentzel, J., van Walsum, T., and Niessen, W., "Coronary lumen segmentation using graph cuts and robust kernel regression," in [*Proc. IPMI 2009*], 528–539 (2009).
- [13] Kirişli, H., Schaap, M., Klein, S., Papadopoulou, S., Bonardi, M., Chen, C., Weustink, A., Mollet, N., Vonken, E. P. A., van der Geest, R., van Walsum, T., and Niessen, W., "Evaluation of a multi-atlas based method for segmentation of cardiac CTA data: a large-scale, multi-center and multi-vendor study," *Medical Physics* **37**(12), 6279–6292 (2010).
- [14] Gupta, V., Hendriks, E., Milles, J., van der Geest, R., Jerosch-Herold, M., Reiber, J., and Lelieveldt, B., "Fully automatic registration and segmentation of first-pass myocardial perfusion mr image sequences," *Academic Radiology* **17**(11), 1375–85 (2010).
- [15] Milles, J., der Geest, R., Jerosch-Herold, M., Reiber, J., and Lelieveldt, B., "Fully automated motion correction in first-pass myocardial perfusion mr image sequences," *IEEE Trans. on Medical Imaging* **27**(11), 1611–1621 (2008).
- [16] Al-Saadi, N., Nagel, E., Gross, M., Bornstedt, A., Schnackenburg, B., Klein, C., Klimek, W., Oswald, H., and Fleck, E., "Noninvasive detection of myocardial ischemia from perfusion reserve based on cardiovascular magnetic resonance," *Circulation* **12**, 1379–1383 (2000).